The Reproduction of the Discovery of Neptune

Mulder, B.

Barbara Mulder

The Reproduction of the Discovery of Neptune

Bachelor thesis

January 19, 2022

Thesis supervisor: dr. E. Sellentin

Leiden University
Mathematical Institute

Contents

1 Introduction

1.1 Background

In the nineteenth century, we only knew about seven planets in the solar system, anything beyond Uranus was unknown territory. In the aftermath of Uranus' discovery in 1781, astronomers observed irregularities in Uranus' orbit around the Sun [1]. Two independent astronomers concluded that a yet undiscovered planet must be the cause. The British mathematician John C. Adams [2] and the French astronomer Urbain Le Verrier [3] both predicted Neptune's location by hand. The latter made the better prediction. Neptune is discovered in 1846 with the aid of a telescope within 1° of his predicted location [3]. Neptune was observed earlier on in the nineteenth century, but it was thought to be some faint star [2]. In this thesis, based on the derivations and structure of [4], we will reproduce the discovery of Neptune with the tools of modern technology.

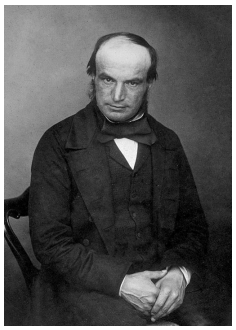

Figure 1: John C. Adams

Figure 2: Urbain Le Verrier

1.2 Goals

We aspire to reproduce the discovery of Neptune using the historical data regarding the irregularities in Uranus' orbit. Using basic celestial mechanics to understand the interaction between the two interfering planets, we formulate a function representing the theoretical perturbation of Uranus by Neptune. We fit this to the historical measured perturbations and hope to be able to accurately predict Neptune's location.

1.3 Outline

In Chapter 2, we introduce some preliminary knowledge. We mainly discuss physics laws that are necessary to describe planetary motion.

In Chapter 3, we consider the forward problem. We first derive an expression for the theoretical perturbation of Uranus by Neptune. In the forward problem, we fit this function to the historical data using the known Neptune characteristics.

In Chapter 4, we consider the inverse problem. In the inverse problem, we also fit the theoretical perturbation to the historical data, but we only use information known at the time of the discovery. From this, we derive Neptune's location.

2 Physics

In this chapter, we discuss the preliminary knowledge relevant throughout this thesis. Predominantly physics laws that are necessary to describe planetary motion in the solar system. We notice that relatively few laws are required to understand how planets move through space. We also illustrate the abnormalities in the orbit of Uranus that eventually led to the discovery of Neptune. This chapter is based on laws described in [1] and [5].

2.1 Notation

First, we introduce some notation to distinguish between vector quantities and scalar quantities. We write vectors in boldface ($\boldsymbol{F}$) and scalars in regular font (m) throughout the thesis. The length of a vector may be written as a scalar or between vertical bars ($|\boldsymbol{x} - \boldsymbol{y}|$), depending on the more legible case.

We will also encounter differential equations with derivatives of vector quantities. For practical reasons we write one dot for the first derivative and two dots for the second derivative with respect to time ($\ddot{\boldsymbol{r}} = \frac{d^2\boldsymbol{r}}{dt^2}$).

2.2 Physics Laws

In order to describe planetary motion, we require some physics. Several laws from Kepler, Newton, and Bode will be featured.

2.2.1 Kepler's Laws

Kepler's three empirical laws regarding planetary motion characterize how planets behave in their orbit around the Sun [1]. These laws are:

1. Each planet moves in an elliptical orbit with the Sun at one of the foci.
2. The line from a planet to the Sun sweeps out equal areas in equal times.
3. The period of a planet squared is proportional to the length of the semi-major axis cubed.

2.2.2 Newton's Law of Gravitation

Newton's law of gravitation states that masses attract each other [5]. This force is calculated as follows:

$$\boldsymbol{F} = -\frac{Gm_1m_2}{|\boldsymbol{r}_1 - \boldsymbol{r}_2|^3}(\boldsymbol{r}_1 - \boldsymbol{r}_2) \tag{1}$$

Where:

- $\boldsymbol{F}$ is the gravitational force planet 2 exerts on planet 1.
- m_1, m_2 are the masses of planet 1 and 2.

- $\boldsymbol{r}_1$, $\boldsymbol{r}_2$ are the positions of planet 1 and 2.
- $|\boldsymbol{r}_1 - \boldsymbol{r}_2|$ is the distance between the centers of planet 1 and 2.
- G is the gravitational constant.

2.2.3 Newton's Second Law

From Newton's famous three laws, we use Newton's second law. This law states that the sum of all forces acting on an object equals the mass times acceleration [5]. Or in short:

$$\sum_i \boldsymbol{F}_i = m\ddot{\boldsymbol{r}} \tag{2}$$

Where:

- m is the mass of the object.
- $\ddot{\boldsymbol{r}}$ is the acceleration of the object.
- $\boldsymbol{F}_i$ is the i'th force acting on the object.

2.2.4 Bode's Law

In the nineteenth century, Bode's law was used to predict the length of the semi-major axis of planets in the solar system [4]. Bode's law states:

$$a = 0.3 \times 2^n + 0.4 \text{ AU} \tag{3}$$

Where:

- a is the semi-major axis of planet with index n in Astronomical Units (AU).
- n is the index corresponding to the planets in the solar system where $n \in \{-\infty, 0, 1, 2, 3, \dots\}$.

At the time, this law seemed to be correct for the known planets, but for Neptune and beyond it fails to predict the length of the semi-major axis. However, we will use this law in order to reproduce the discovery of Neptune.

2.3 Astrophysical Concepts

In astronomy, one deals with great distances and masses but with small angles and discrepancies. Therefore, the regular SI-units are not always convenient. We introduce several useful units and concepts from [1] used throughout the following chapters.

2.3.1 Units

The following units are used instead of the usual SI-units for angles, distances, and masses.

- An arcsecond ($''$) is $\frac{1}{3600}$ of a degree.
- An Astronomical Unit (AU) is the average distance between the Earth and the Sun.
- A solar mass ($m_\odot$) is the mass of the Sun.

2.3.2 Ecliptic

The vast majority of planets in the solar system move in approximately the same plane. The plane in which the Earth orbits the Sun is referred to as the ecliptic [1]. The trajectory of most other planets only have a slight inclination with respect to this plane. Hence, we refer to the ecliptic as the approximate plane in which all planets orbit the Sun.

2.3.3 Longitude and Latitude

In order to specify positions in the sky, we use heliocentric longitudes and latitudes [1]. Latitude is measured as the angle between the ecliptic and the line connecting the position of the celestial body and the Sun's center. Latitudes to the south are negative. Longitude is measured as the angle between the vernal equinox and the line connecting the position of the celestial body and the Sun's center. An equinox is the line through the Sun and the Earth when it is parallel to the equator plane. This phenomenon occurs twice a year, once in September and once in March. The March equinox is referred to as the vernal equinox. Longitudes to the west are negative.

2.4 Equation of Motion of a Three-Body System

The equation of motion is the differential equation we obtain when substituting all forces interfering with our object into Newton's second law [5]. Solving this equation yields the position, velocity, and acceleration of an object in time. We consider a three-body system. We sum the gravitational forces between the three celestial bodies and use Newton's second law. This results in the following equation [4]:

$$\ddot{\boldsymbol{r}}_i = -G \sum_{j \neq i}^{3} \frac{m_j}{|\boldsymbol{r}_i - \boldsymbol{r}_j|^3} (\boldsymbol{r}_i - \boldsymbol{r}_j) \tag{4}$$

Using this equation, we can predict the path of a planet if only two other celestial objects are interfering with its trajectory.

2.5 Perturbations of Uranus

When observing Uranus' orbit between the eighteenth and nineteenth century, one noticed that Uranus moved in a peculiar way. It did not behave according to Kepler's laws [4]. Its orbit was sometimes ahead or behind its predicted course. At the time, there were few theories that could explain the irregularities in Uranus' orbit. Scientists considered that perhaps the Sun's gravity differs at great distances or that it might be observational errors [3]. Neither turned out to be the case. Another theory was that the planet was being pulled out of its orbit by a yet unknown mass in or near the solar system [4]. Thus, there might be another planet in the solar system. This turned out to be the case. We now know this planet as Neptune.

2.5.1 Neptune's Influence

To visualize the perturbations in Uranus' orbit, we first consider the force field of a single planet. A force field is a vector field in which the arrows represent the direction and magnitude of the force an object would experience at that specific location [5]. In Figure 3, we see the force field of one planet. The planet is located at $(5, 5)$.

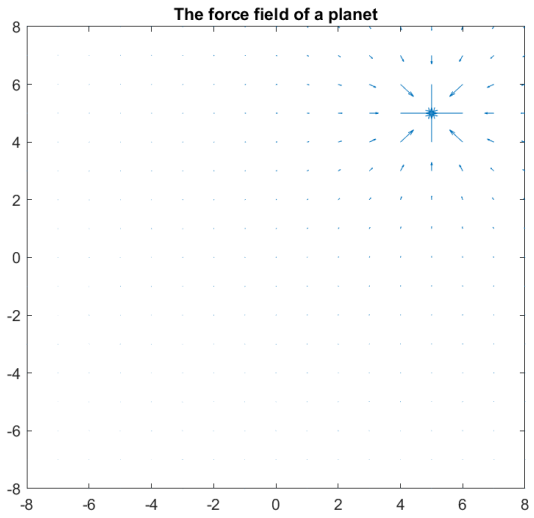

Figure 3: The force field of one single planet located at $(5, 5)$. The arrows represent the direction and magnitude of the force an object would experience at that specific location.

Nearby the planet an object is pulled towards the planet, but at greater distances we can neglect this force. From Neptune's force field, we can visualize how Uranus' perturbations originate. We consider the force field of one planet again,

this represents the force field caused by Neptune. In Figure 4, we see the force field of Neptune and the orbit of Uranus.

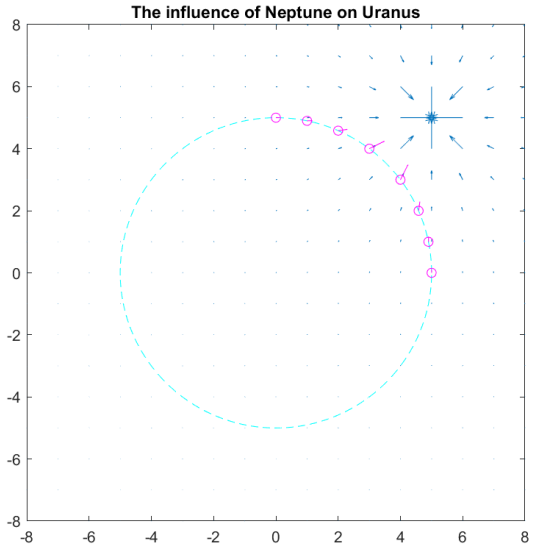

Figure 4: A graphical representation of the influence of Neptune on Uranus' orbit. The blue circle represents Uranus' orbit and the purple circles represent Uranus at different moments in time. The purple arrows from these circles are the forces Uranus experiences due to the gravitational force of Neptune.

The blue circle represents Uranus' orbit and the small purple circles represent Uranus at different moments in time. The arrows from these purple dots represent the force that Neptune exerts on Uranus. We see that Uranus is pulled towards Neptune. If we imagine Uranus moving counterclockwise, we observe at the right side of the orbit that Uranus is pulled ahead in its orbit and at the top it is pulled back in its orbit. This is what caused the observed irregularities in Uranus' orbit by Neptune.

2.5.2 Discrepancy

The perturbations of Uranus are referred to as the discrepancy in longitude. The discrepancy $\Delta\phi$ is the remaining discrepancy in longitude of Uranus after subtracting other planetary perturbations [4]. Hence, $\Delta\phi$ is the discrepancy caused by the unknown mass we are looking for. The remaining discrepancy $\Delta\phi$ is shown in Figure 5 in arcseconds. The data can be found in [4].

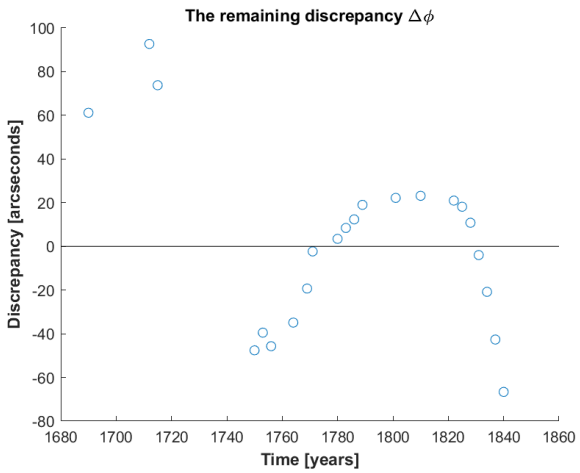

Figure 5: The measured discrepancy $\Delta\phi$ in arcseconds after subtracting other planetary perturbations. Thus, $\Delta\phi$ is the remaining discrepancy caused by Neptune. The table with this data can be found in [4].

3 Forward Problem

Prior to predicting Neptune's location from the remaining discrepancy, we consider the forward problem introduced in [4]. In the forward problem, we use the known Neptune characteristics to determine the theoretical discrepancy. This theoretical discrepancy will be useful in the reverse case, where we calculate the Neptune characteristics from the historically measured perturbations. All assumptions, derivations, notation and solutions in the following two subsections stem from the forward problem discussed in [4].

3.1 The Equation of Motion

In order to derive the theoretical discrepancy, denoted $\Delta\phi_{th}$ [4], we take a closer look at the orbit of Uranus. We want to be able to describe its location, velocity, and acceleration at any moment in time. We accomplish this by solving the equation of motion of a three-body system. We start by simplifying the problem and formulate Uranus' equation of motion. Subsequently, we solve these equations to obtain $\Delta\phi_{th}$.

3.1.1 Assumptions

Since $\Delta\phi$ is the remaining discrepancy, we only consider a three-body system with the Sun, Uranus, and Neptune. The orbits of these planets are nearly circular. We neglect these small eccentricities and assume that all three orbits are perfect circles. Furthermore, we assume that the radii of the orbits are equal to the length of the semi-major axis. Since it does not differ much from the semi-minor axis, this is just a matter of choice. Also, we assume that the three planets move in the same plane. Hence, we neglect the small inclinations with respect to the ecliptic.

3.1.2 Perturbed and Unperturbed Motion

Before we describe the perturbed and unperturbed motion of Uranus, we introduce some notation useful throughout the thesis. The subscripts U, N, and $\odot$ refer to Uranus, Neptune, and the Sun. The following constants regarding the three celestial bodies will appear in the upcoming chapters:

- *Radii*: R_U, R_N and $R_\odot$ in AU.
- *Mass*: m_U, m_N and $m_\odot$ in solar masses i.e. $m_\odot = 1$.
- *Orbital period*: T_U and T_N in years.
- *Angular frequency*: $\Omega_U = \frac{2\pi}{T_U}$ and $\Omega_N = \frac{2\pi}{T_N}$ in radians per year.

Define $t_0 = 1822$ to be the time of conjunction [4]. The time of conjunction is the year in which Uranus, Neptune and the Sun align. To visualize the motion of the two planets around the Sun, observe Figure 6. It depicts Uranus and

Neptune with their respective orbits. Both planets are moving counterclockwise around the Sun. In the figure, the time of conjunction occurs when the three celestial bodies are on the x-axis.

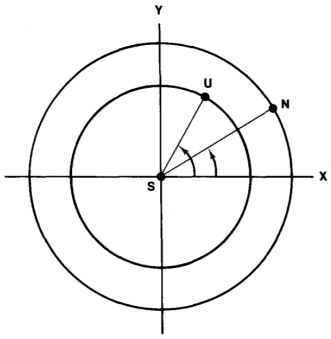

Figure 6: The unperturbed motion of Uranus (U) and Neptune (N). The two planets move counterclockwise in their respective orbits around the Sun (S) located at the center. The figure can be found in [4].

In [4], they switch to a more convenient time scale $\tau = t - t_0$. Consequently, $\tau = 0$ during the time of conjunction.

To envision the perturbations, they change to a rotating frame with angular frequency Ω_U. In this frame, depicted in Figure 7, Uranus would be stationary without the perturbations. Neptune on the other hand is moving with an angular frequency $-\Omega$, where Ω is defined as $\Omega = \Omega_U - \Omega_N$. The minus sign informs us it is moving clockwise.

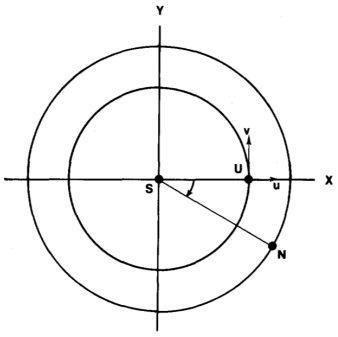

Figure 7: The perturbed motion of Uranus in the frame rotating with Ω_U. In this frame, Uranus is only showing its perturbations u and v. Uranus would be stationary without the perturbations. Neptune moves clockwise with angular frequency $\Omega = \Omega_U - \Omega_N$. The figure can be found in [4].

As stated earlier, Uranus is only showing its perturbations in this frame. We define the perturbation in the x-direction as $u(\tau)$ and the perturbation in the

y-direction as $v(\tau)$. This implies that u is the radial deviation and $\frac{v}{R_U} = \Delta\phi$ is the deviation in longitude. To grasp why the latter is true, consider $\angle USv$. In Figure 7, $\angle USv = \Delta\phi$ is the perturbation in longitude caused by Neptune [4]. We know $\tan(\Delta\phi) = \frac{v}{R_U}$. Using the small angle approximation, $\tan(\Delta\phi) \approx \Delta\phi$, yields $\Delta\phi = \frac{v}{R_U}$.

From these observations, they deduce the perturbed and unperturbed solutions using polar coordinates [4]:

- *Unperturbed motion*: $\tilde{\rho}(\tau) = R_U$ and $\tilde{\phi}(\tau) = \Omega_U \tau$.
- *Perturbed motion*: $\rho(\tau) = R_U + u(\tau)$ and $\phi(\tau) = \Omega_U \tau + \frac{v(\tau)}{R_U}$.

For the remainder of the chapters, we will only be interested in deriving the perturbations in longitude. We lack the data regarding the radial perturbations, since radial perturbations are hard to measure [4]. Therefore, we do not take it into consideration.

3.1.3 Deriving the Equation of Motion

We follow the derivation of the equation of motion as in [4]. We start by introducing heliocentric coordinates. In other words, sun-centered coordinates:

$$\boldsymbol{\rho}_i = \boldsymbol{r}_i - \boldsymbol{r}_\odot \tag{5}$$

where $i \in \{\text{N,U,}\odot\}$. Thus, the equation of motion as previously discussed becomes:

$$\ddot{\boldsymbol{\rho}_U} = -\ddot{\boldsymbol{r}}_\odot - G \sum_{j=N,S} \frac{m_j}{|\boldsymbol{\rho}_U - \boldsymbol{\rho}_j|^3}(\boldsymbol{\rho}_U - \boldsymbol{\rho}_j) \tag{6}$$

where $\ddot{\boldsymbol{r}}_\odot$ is called the *pseudo acceleration*. This term is the result of choosing a non-inertial frame of reference i.e. a frame undergoing acceleration. We calculate the *pseudo acceleration* as follows:

$$\ddot{\boldsymbol{r}}_\odot = -G \sum_{j=U,N} \frac{m_j}{|0 - \boldsymbol{\rho}_j|^3}(0 - \boldsymbol{\rho}_j) = G\left(\frac{m_U}{(\rho_U)^3}\boldsymbol{\rho}_U + \frac{m_N}{(\rho_N)^3}\boldsymbol{\rho}_N\right) \tag{7}$$

We substitute $\ddot{\boldsymbol{r}}_\odot$ into the equation of motion, which results in:

$$\ddot{\boldsymbol{\rho}}_U + G(m_S + m_U)\frac{\boldsymbol{\rho}_U}{\rho_U^3} = Gm_N\left(\frac{\boldsymbol{\rho}_N - \boldsymbol{\rho}_U}{|\boldsymbol{\rho}_N - \boldsymbol{\rho}_U|^3} - \frac{\boldsymbol{\rho}_N}{\rho_N^3}\right) = \frac{Gm_N}{R_N^2}\boldsymbol{F} = \epsilon\boldsymbol{F} \tag{8}$$

where $\epsilon\boldsymbol{F}$ with $\epsilon = \frac{Gm_N}{R_N^2}$ is the total force that the Sun and Neptune exert on Uranus. Using polar coordinates, the equation of motion separates into the following two differential equations:

$$\ddot{\rho} - \rho\dot{\phi}^2 + \frac{G(m_S + m_U)}{\rho^2} = \epsilon F_r \tag{9}$$

$$\rho\ddot{\phi} + 2\dot{\rho}\dot{\phi} = \epsilon F_\phi \tag{10}$$

where F_r and F_ϕ are the r- and ϕ-components of $\boldsymbol{F}$.

Recall the perturbed motion of Uranus and compute the derivatives:

- $\rho(\tau) = R_U + u(\tau)$, where $\dot{\rho}(\tau) = \dot{u}(\tau)$ and $\ddot{\rho}(\tau) = \ddot{u}(\tau)$.
- $\phi(\tau) = \Omega_U\tau + \frac{v(\tau)}{R_U}$, where $\dot{\phi}(\tau) = \Omega_U + \frac{\dot{v}(\tau)}{R_U}$ and $\ddot{\phi}(\tau) = \frac{\ddot{v}(\tau)}{R_U}$.

Substituting the perturbed solution in the differential equations and simplifying them yields:

$$\ddot{u} - 2\Omega_U\dot{v} - 3\Omega_U^2 u = \epsilon F_r \tag{11}$$

$$\ddot{v} + 2\Omega_U\dot{u} = \epsilon F_\phi \tag{12}$$

Solving these equations provides us with the theoretical discrepancy $\Delta\phi_{th}$. We refer to [4] for a more detailed derivation of the above equations of motion.

3.2 Solving the Equation of Motion

When solving differential equations, we look for the homogeneous solution and the inhomogeneous solution. Recall that the solution of differential equations is the sum of the homogeneous and inhomogeneous solutions. We begin with the homogeneous equations. A more detailed derivation of both solutions can be found in [4].

3.2.1 Homogeneous Solution

The homogeneous equations of motion are merely the regular equations of motions, except we set $\boldsymbol{F} = 0$. Hence:

$$\ddot{u} - 2\Omega_U\dot{v} - 3\Omega_U^2 u = 0 \tag{13}$$

$$\ddot{v} + 2\Omega_U\dot{u} = 0 \tag{14}$$

The solutions to this system of differential equations stem from the normal modes or the natural frequencies 0 and Ω_U. The solutions for both normal modes are outlined below.

The solution for natural frequency 0 is:

- $u = -\frac{2}{3}\alpha_1$
- $v = \alpha_1\Omega_U\tau + \alpha_2$

The solution for natural frequency Ω_U is:

- $u = -\frac{1}{2}\alpha_3\cos(\Omega_U\tau) + \frac{1}{2}\alpha_4\sin(\Omega_U\tau)$
- $v = \alpha_3\sin(\Omega_U\tau) + \alpha_4\cos(\Omega_U\tau)$

One can easily verify these are the solutions to the homogeneous equations.

3.2.2 Inhomogeneous Solution

Prior to solving the inhomogeneous equation of motion, we take a closer look at ϵF_r and ϵF_ϕ, which are the r- and ϕ-components of:

$$\epsilon \boldsymbol{F} = G m_N \left(\frac{\boldsymbol{\rho}_N - \boldsymbol{\rho}_U}{|\boldsymbol{\rho}_U - \boldsymbol{\rho}_N|^3} - \frac{\boldsymbol{\rho}_N}{\rho_N^3} \right) \tag{15}$$

where $\boldsymbol{\rho}_U = (R_U, 0)$ and $\boldsymbol{\rho}_N = (R_N \cos(\Omega\tau), -R_N \sin(\Omega\tau))$. If we substitute these expressions in equation (15), we obtain:

$$F_r = \frac{\cos(\Omega\tau) - k}{(1 - 2k\cos(\Omega\tau) + k^2)^{3/2}} - \cos(\Omega\tau) \tag{16}$$

$$F_\phi = \frac{-\sin(\Omega\tau)}{(1 - 2k\cos(\Omega\tau) + k^2)^{3/2}} + \sin(\Omega\tau) \tag{17}$$

where $k = \frac{R_U}{R_N}$. We leave out the ϵ term. In Figure 8 below, we see one oscillation of both F_r and F_ϕ. We immediately observe that F_r is an even function and F_ϕ an odd function. Both are not purely sinusoidal. Therefore, they must contain harmonics at frequencies $n\Omega$ for $n \in \mathbb{N}$.

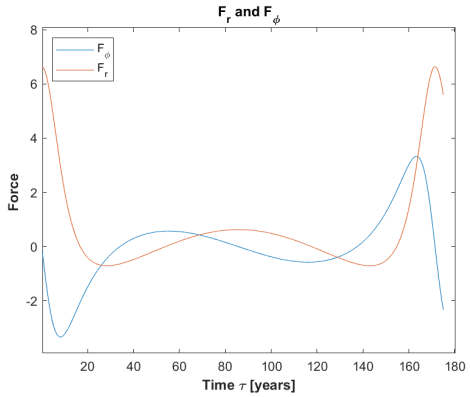

Figure 8: One oscillation of F_r and F_ϕ. These are the r- and ϕ-components of $\boldsymbol{F}$, where $\epsilon\boldsymbol{F}$ is the total force the Sun and Neptune exert on Uranus.

In order to find dominating terms, we describe F_r and F_ϕ using Fourier series. We conclude that they must be of the following form given the observed parity:

- $F_r = \sum_{n=0}^{\infty} a_n \cos(n\Omega\tau)$
- $F_\phi = \sum_{n=0}^{\infty} b_n \sin(n\Omega\tau)$

Recall that we can determine all a_n and b_n as follows:

$$a_n = \frac{1}{2\pi} \int_0^{2\pi} F_r \cos(n\Omega\tau) d(\Omega\tau) \tag{18}$$

$$b_n = \frac{1}{2\pi}\int_0^{2\pi} F_\phi \sin(n\Omega\tau)d(\Omega\tau) \tag{19}$$

If we substitute the expressions for F_r and F_ϕ in our equations of motions, we conclude that u and v must be of the following form:

- $u = \epsilon \sum_{n=0}^{\infty} u_n \cos(n\Omega\tau)$
- $v = \epsilon \sum_{n=0}^{\infty} v_n \sin(n\Omega\tau)$

Substituting u and v into the equations of motion gives us expressions for the u_n's and v_n's. For $n \geq 1$, we have:

$$v_n = \frac{-2n\Omega\Omega_U a_n + (3\Omega_U^2 + n^2\Omega^2)b_n}{n^2\Omega^2(\Omega_U^2 - n^2\Omega^2)} \tag{20}$$

$$u_n = \frac{n\Omega a_n - 2\Omega_U b_n}{n\Omega(\Omega_U^2 - n^2\Omega^2)} \tag{21}$$

with $u_0 = -\frac{a_0}{3\Omega_U^2}$ and $v_0 = 0$. Since these are elaborate expressions, we look for dominating terms. We do this by searching for resonant terms. Resonance occurs when the driving frequency is near the resonance frequency. In our case, the driving frequency is $n\Omega$ and the resonance frequency is Ω_U. Thus, we search for the $n \in \mathbb{N}$ such that $\Omega_U \approx n\Omega$. In this case, the denominator of v_n is close to zero, resulting in large values for v_n. Therefore, this term must dominate.

This turns out to be the case for $n = 2$. For $n \in \mathbb{N} \setminus \{2\}$, the result is at least one order of magnitude smaller and hence we neglect them. We conclude that the inhomogeneous solution is:

$$v_{inhom} = \epsilon \sum_{n=0}^{\infty} v_n \sin(n\Omega\tau) \approx \epsilon v_2 \sin(2\Omega\tau). \tag{22}$$

where $\epsilon v_2 = -\gamma = -4.32 \times 10^{-3}$ rad$= 890''$. Since the measured discrepancy is in the range 0 - 100 arcseconds, we suspect that γ is a factor too large.

3.2.3 Complete Solution

For the complete solution, we sum the solutions to the homogeneous and inhomogeneous equations. Or in short:

$$\Delta\phi_{th} = \frac{v_{inhom}}{R_U} + \frac{v_{hom}}{R_U} \tag{23}$$

In which we substitute the foregoing solutions:

- $v_{hom,0} = \alpha_1\Omega_U\tau + \alpha_2$
- $v_{hom,\Omega_U} = \alpha_3 \sin(\Omega_U\tau) + \alpha_4 \cos(\Omega_U\tau)$
- $v_{inhom} = \epsilon v_2 \sin(2\Omega\tau)$

Substituting these solutions yields the following expression for the theoretical discrepancy in longitude:

$$\Delta\phi(\tau) = -\gamma \sin(2\Omega\tau) + \beta_1\Omega_U\tau + \beta_2 + \beta_3 \sin(\Omega_U\tau) + \beta_4 \cos(\Omega_U\tau) \tag{24}$$

where $\beta_i = \frac{\alpha_i}{R_U}$ and $-\gamma = \epsilon v_2$. For a more detailed derivation of $\Delta\phi_{th}$, we refer one to [4].

3.3 Fitting the Data Using $\Delta\phi_{th}$

In this section, we fit the theoretical discrepancy $\Delta\phi_{th}$ from [4] to the historical data. In this manner, we can find the optimal values for β_i with $i \in \{1, 2, 3, 4\}$. We execute the fits with the known time of conjunction t_0, the theoretical γ, and once where we vary both parameters. Furthermore, we consider the error between the observed discrepancy and the theoretical discrepancy regarding these various cases. This way one can truly compare the cases. We use the root-mean-square error (D^2 or RMS) introduced in [4] to accomplish this. The fit function is simply $\Delta\phi_{th}$, in which we substituted the known Neptune parameter $\Omega = \Omega_U - \Omega_N$:

$$\Delta\phi_{th}(t) = -\gamma \sin(2\Omega(t-t_0))+\beta_1\Omega_U(t-t_0)+\beta_2+\beta_3 \sin(\Omega_U(t-t_0))+\beta_4 \cos(\Omega_U(t-t_0)) \tag{25}$$

3.3.1 Vary t_0

We start by comparing the fitted $\Delta\phi_{th}$ for different values of t_0. In Figure 9, we see the results for values of t_0 between 1800 and 1840. Evidently, the values close to 1822 seem to allow a closer fit to the data. The fit with $t_0 = 1830$ might even agree more with data than $t_0 = 1820$.

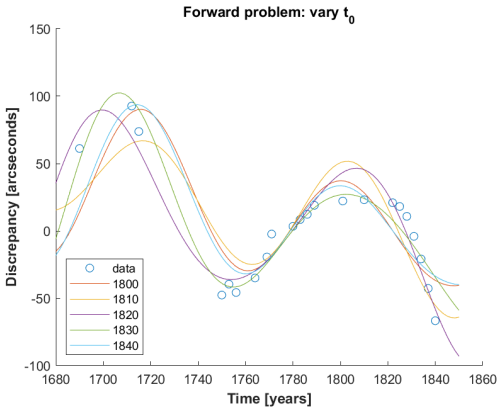

Figure 9: $\Delta\phi_{th}$ fitted to the historical data for different values of t_0 between 1800 and 1840. The curve with $t_0 = 1830$ seems the closest fit.

We continue with the actual time of conjunction and compare this with other values close to $t_0 = 1822$. We compare the results in Figure 10.

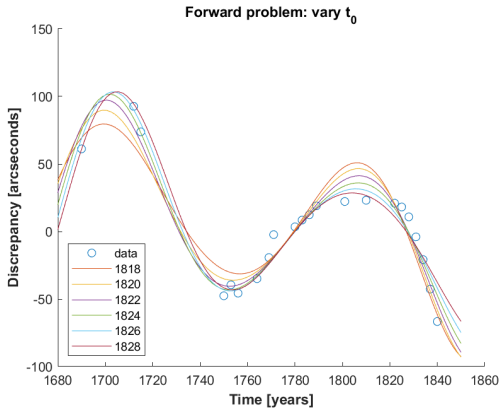

Figure 10: $\Delta\phi_{th}$ fitted to the historical data for different values of t_0 close to the actual time of conjunction $t_0 = 1822$. We fitted $\Delta\phi_{th}$ for values of t_0 between 1818 and 1828. The curves between 1822 and 1828 seem the closest fits. Thus, the optimal value for t_0 might be later than 1822.

We observe that the overall form of the plots are similar, but around $t_0 = 1822$ the fits resemble the data more than for other years. This is in line with our expectations, but we conclude that a few years more or less does not drastically change the fit. A few years later might even allow for a better fit to the data.

3.3.2 Vary γ

We continue with the second case, where we compare the theoretical value $\gamma_{th} = 890''$ with different values of γ. We first consider $\Delta\phi_{th}$ for different values of γ. In this case we fix $t_0 = 1822$. The results are plotted in Figure 11. We observe that γ between $500''$ and $700''$ allows for the closest fits. Therefore, we conclude that $\gamma_{th} = 890''$ must be too large.

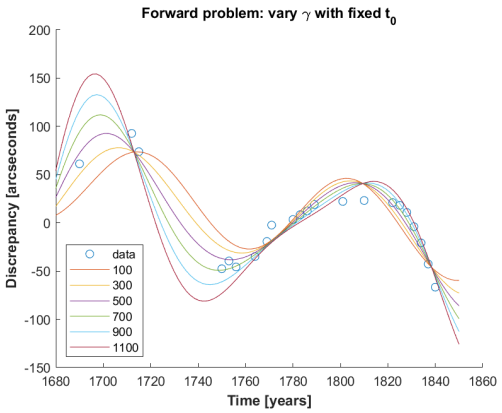

Figure 11: $\Delta\phi_{th}$ fitted to the historical data for different values of γ between 100 and 1100. The curve with $\gamma = 500''$ seems the closest fit. The theoretical $\gamma_{th} = 890''$ is probably too large.

We continue with the following three cases:

1. We fix both $\gamma_{th} = 4.32 \times 10^{-3}$ rad $= 890''$ and $t_0 = 1822$.
2. We vary γ and fix $t_0 = 1822$.
3. We fix $\gamma_{th} = 4.32 \times 10^{-3}$ rad $= 890''$ and vary t_0.

We fitted the three preceding situations to the data and obtained the results displayed in Figure 12. Case two, where we varied γ, is the best fit to the data. This is in line with our expectations since the theoretical γ_{th} was a factor larger than the observed perturbations. We obtained $\gamma = 550.3649''$ in the second case. Indeed, lower than the theoretical $\gamma_{th} = 890''$, but bigger than the measured discrepancy.

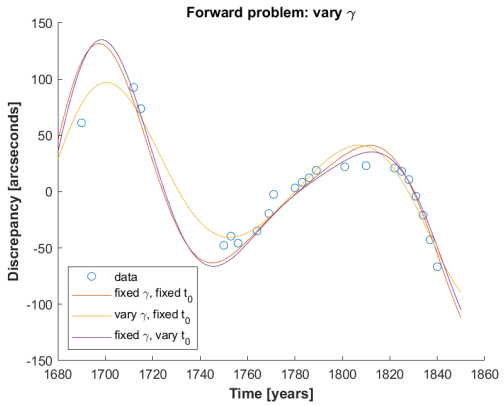

Figure 12: $\Delta\phi_{th}$ fitted to the historical data for the three different scenarios discussed previously. We clearly observe that using $\gamma_{th} = 890''$ obtains a worse result than varying γ. Varying t_0 on the other hand does not improve the result much.

Furthermore, we see little distinction between the other two cases. Since the fixed $t_0 = 1822$ is the actual time of conjunction, varying t_0 should not make a big difference, which is displayed in the figure. In the third case, we obtained $t_0 = 1823.3955$.

3.3.3 Vary All

In this last section, we vary both parameters t_0 and γ. In Figure 13, the outcome is plotted. We see that the plot is really consistent with the data. In this case, we have $\gamma = 541.9447''$ and $t_0 = 1824.7048$.

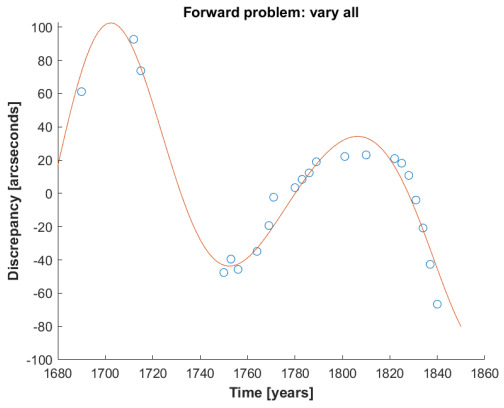

Figure 13: $\Delta\phi_{th}$ fitted to the historical data where we vary both γ and t_0.

We compare this result to the results from the previous section. Thus, we plot

the case where $t_0 = 1822$, the case where $\gamma_{th} = 890''$, and the plot from the preceding figure. In Figure 14, we observe these three cases.

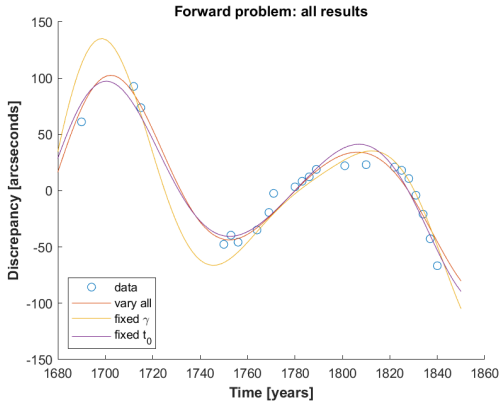

Figure 14: $\Delta\phi_{th}$ fitted to the historical data with fixed γ, fixed t_0 or varied γ and t_0. Using $\gamma_{th} = 890''$ prevents us from getting a close fit to the data. The other two cases are similar, but varying both γ and t_0 allows for the closest fit.

We compare the three results and observe that the best fit to the forward problem is the one where we varied both t_0 and γ. Obviously, having fewer constraints allows for a better fit. Comparing it to the other two cases, we see that γ_{th} must be too large. Varying t_0 does not influence the result considerably.

3.4 Root-Mean-Square Errors

In this section, we calculate the error between the fit and the original data for the three cases previously discussed. We use the root-mean-square error to accomplish this. The root-mean-square error is defined as follows:

$$D^2 = \frac{1}{N}\sum_{i=1}^{N}[\Delta\phi(\tau_i) - \Delta\phi_{th}(\tau_i)]^2 \tag{26}$$

where $\Delta\phi(\tau_i)$ are the observed remaining discrepancies in Uranus' orbit and $\Delta\phi_{th}(\tau_i)$ the fitted function value at time τ_i. This expression for the root-mean-square error can be found in [4].

3.4.1 Vary t_0

We start with calculating the root-mean-square error of the fit for different times of conjunction. We vary γ in this section. The root-mean-square error for different values of t_0 is plotted in Figure 15.

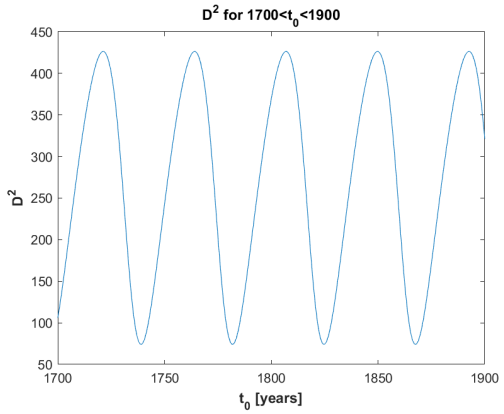

Figure 15: The root-mean-square error D^2 for different values of t_0 where for every t_0 the discrepancy $\Delta\phi_{th}$ is fitted to the data. The error is periodic and the minimum closest to 1822 is $D^2 = 74.0006$ at $t_0 = 1824.7048$.

We observe that the error is periodic and attains it minimum every few years. This is expected, since the fit function $\Delta\phi_{th}$ a summation of trigonometric functions. A minimum of D^2 closest to 1822 is attained at $t_0 = 1824.7048$, where $D^2 = 74.0006$. The minimum is thus reached a few years after the actual time of conjunction.

At $t_0 = 1822$ the error is $D^2 = 94.9520$, a significant difference compared to the global minimum of D^2.

3.4.2 Vary γ

In this section, we compare the error for the three cases of γ.

1. In the first case, where we fixed both t_0 and γ, the error is $D^2 = 221.1766$.
2. For the second case, where we varied γ and fixed t_0, we plot the error against γ. Examine Figure 16.

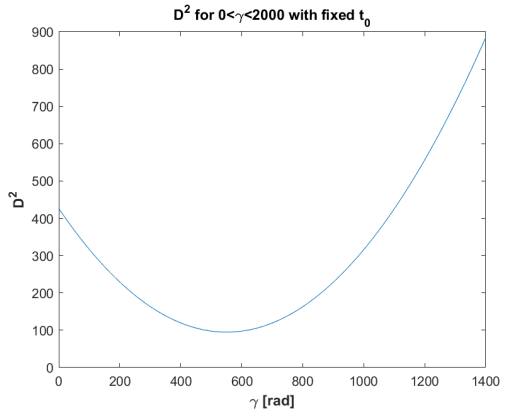

Figure 16: The root-mean-square error D^2 for different values of γ where for every γ the discrepancy $\Delta\phi_{th}$ is fitted to the data. We fixed $t_0 = 1822$. The error is parabola shaped and the minimum is $D^2 = 94.9520$ attained at $\gamma = 550.3649''$.

We observe a parabola shaped error plot, which eventually keeps on increasing in γ. The error plot attains its minimum at $\gamma = 550.3649''$, where $D^2 = 94.9520$.

3. We pursue with the third case, where we fixed $\gamma_{th} = 890''$ and varied t_0. In Figure 17, we plotted the error against t_0.

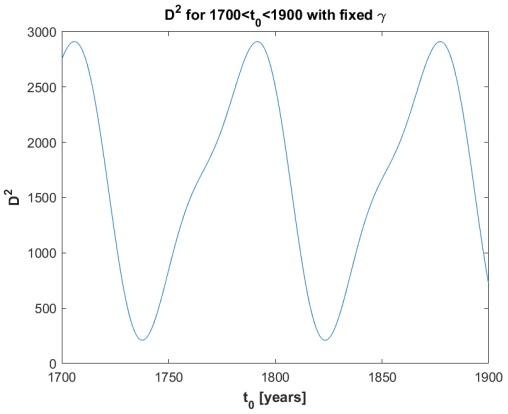

Figure 17: The root-mean-square error D^2 for different values of t_0 where for every t_0 the discrepancy $\Delta\phi_{th}$ is fitted to the data. We fixed $\gamma_{th} = 890''$. The error is periodic and the minimum closest to 1822 is $D^2 = 209.4250$ at $t_0 = 1823.4$.

Once more, we have a periodic D^2 with respect to t_0. The minimum value for the error is $D^2 = 209.4250$, where $t_0 = 1823.4$.

From the values of D^2 of the previous cases, we conclude that in particular using γ_{th} prevents us from obtaining a better fit to the forward problem. Varying t_0 has a less drastic effect on the root-mean-square error.

3.4.3 Vary All

In this last section, we consider the error when we varied both γ and t_0. In Figure 18, we observe the error plotted against t_0.

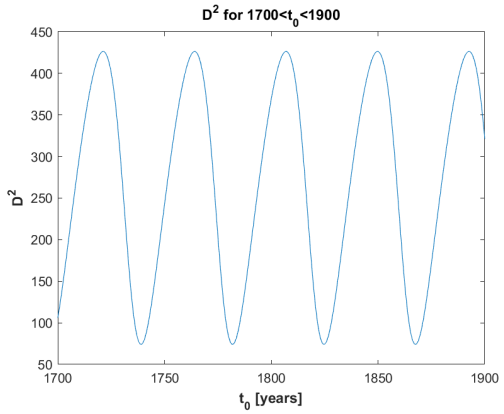

Figure 18: The root-mean-square error D^2 for different values of t_0 where for every t_0 the discrepancy $\Delta\phi_{th}$ is fitted to the data. The error is periodic and the minimum closest to 1822 is $D^2 = 74.0006$ at $t_0 = 1824.7048$.

We observe a sinusoidal error plot. This is always the case when observing the error of different values of t_0. A minimum of D^2 is attained at $t_0 = 1824.7048$. In Figure 19, we plotted the error against γ.

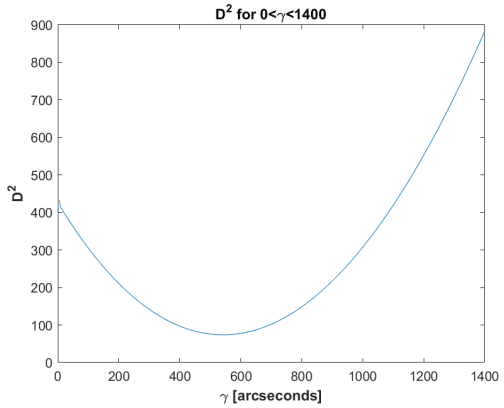

Figure 19: The root-mean-square error D^2 for different values of γ where for every γ the discrepancy $\Delta\phi_{th}$ is fitted to the data. We varied t_0. The error is parabola shaped and the minimum is $D^2 = 74.0006$ attained at $\gamma = 541.9447''$.

Here, the minimum for D^2 is attained at $\gamma = 541.9447''$. The minimum error is $D^2 = 74.0006$. This is the smallest error we have encountered. Therefore, this is the best fit to the forward problem.

3.5 Conclusion Forward Problem

Using the equation of motion of a three-body system, we derived a system of differential equations for the perturbations in the radial and ϕ-direction. We solved these equations and obtained an expression for $\Delta\phi_{th}$ [4]. We proceeded with fitting this theoretical discrepancy to the historical data. We concluded that a later time of conjunction agrees a bit better with the data and that the theoretical γ is a factor too large. The best fit to the forward problem is obtained when varying both γ and t_0. We obtained $t_0 = 1824.7048$ and $\gamma = 541.9447''$, with error $D^2 = 74.0006$. Changes in γ seemed to have the greatest impact on the D^2 error. In the forward problem discussed in [4], the result for D^2 is lower, namely, $D^2 = 11.1$. This is probably due to the fact that back in the day it was sufficient to use Bézier curves or other techniques to make plots agree with the data. For example, they might have taken a wire and bent it until they were satisfied. It seems that they used such a technique to obtain a lower D^2 error than we did.

4 Inverse Problem

In this chapter, we consider the inverse problem introduced in [4]. In this case, we assume we only know the observed perturbations and Uranus' characteristics. We do not use any known information about Neptune. We start by fitting the theoretical discrepancy $\Delta\phi_{th}$ to the data using Bode's law [4]. We also vary Ω_N to the data. Subsequently, we calculate the root-mean-square error for both these cases and finally deduce Neptune's predicted location.

4.1 Bode's Law

In the nineteenth century, the approximate distance to a planet was calculated using Bode's law [4]. As discussed earlier, this law is correct up to Uranus but fails to predict the distance to Neptune. Nevertheless, since astronomers used this method at the time, we also use this law in order to reproduce the discovery of Neptune.

4.2 Fitting the Data Using $\Delta\phi_{th}$

Recall the theoretical discrepancy derived in the forward problem:

$$\Delta\phi_{th}(\tau) = -\gamma\sin(2\Omega\tau) + \beta_1\Omega_U\tau + \beta_2 + \beta_3\sin(\Omega_U\tau) + \beta_4\cos(\Omega_U\tau) \tag{27}$$

We fit this to the data in a similar way as we did in the forward problem. We start by using Bode's law [4] to derive Ω_{Bode}.

4.2.1 Using Ω_{Bode}

First, we use Bode's law [4] to calculate the presumed distance to Neptune. Since $n = 6$ corresponds to Uranus, we use $n = 7$ for Neptune, which provides us with $R_{N,Bode}$:

$$R_{N,Bode} = 0.3 \times 2^7 + 0.4 = 38.8 \text{ AU} \tag{28}$$

We apply Kepler's third law, namely $T^2 \propto R^3$, to calculate $T_{Bode,N}$. We observe for all planets prior to Neptune that $T^2 \approx R^3$ with R in AU and T in years. We obtain:

$$T_{N,Bode} \approx R_{N,Bode}^{\frac{3}{2}} = 241,684 \text{ years} \tag{29}$$

From this and and the fact that $\Omega = \frac{2\pi}{T}$, we calculate:

$$\Omega_{N,Bode} = \frac{2\pi}{T_{N,Bode}} = 2,59975 \cdot 10^{-2} \text{ radians per year} \tag{30}$$

Finally, we calculate Ω_{Bode}:

$$\Omega_{Bode} = \Omega_U - \Omega_{N,Bode} = 4,879 \cdot 10^{-2} \text{ radians per year} \tag{31}$$

Notice that all these results differ quite a bit from the actual Neptune constants. Substituting Ω_{Bode}, yields the following function to fit the data:

$$\Delta\phi_{th}(\tau) = -\gamma sin(2\Omega_{Bode}\tau) + \beta_1\Omega_U\tau + \beta_2 + \beta_3 sin(\Omega_U\tau) + \beta_4 cos(\Omega_U\tau) \quad (32)$$

We first consider different values for Neptune's mass and compare the fits. This is equivalent to varying γ, since $\gamma \propto \epsilon \propto m_N$. In Figure 20, we plotted the fitted function for different values of γ.

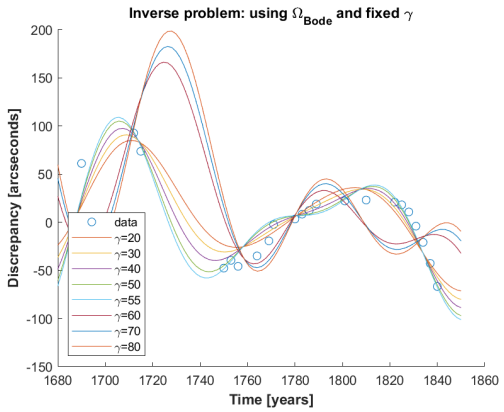

Figure 20: $\Delta\phi_{th}$ with Ω_{Bode} fitted to the historical data for different values of γ between 20 and 80. The curve with $\gamma = 50''$ seems the closest fit. Between $\gamma = 55''$ and $\gamma = 60''$ the overall look of the plots change drastically.

From Figure 20, we conclude that around $\gamma \approx 50''$ the fit seems the most consistent with the data. Furthermore, the overall look of the plot changes drastically between $55''$ and $60''$. Beyond this value, the plots are not consistent with the data anymore. Therefore, we expect the error to change drastically as well. Secondly, we examine the fits for different values of t_0. In Figure 21, we plotted the fitted function for different values of t_0.

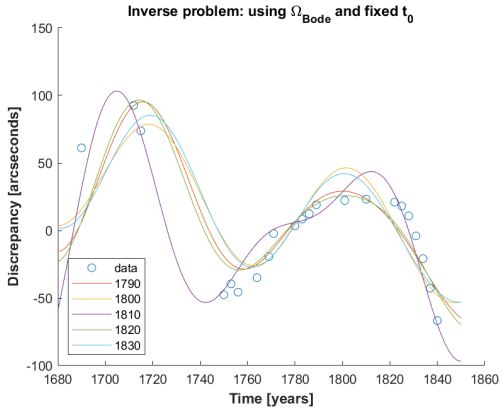

Figure 21: $\Delta\phi_{th}$ with Ω_{Bode} fitted to the historical data for different values of t_0 close to the actual time of conjunction $t_0 = 1822$. We fitted $\Delta\phi_{th}$ for values of t_0 between 1790 and 1830. The curve with $t_0 = 1810$ is the closest fit. The other curves look different but similar to each other.

We clearly see that $t_0 \approx 1810$ allows for the closest fit to the data. Finally, we vary both γ and t_0. This results in the following fit in Figure 22:

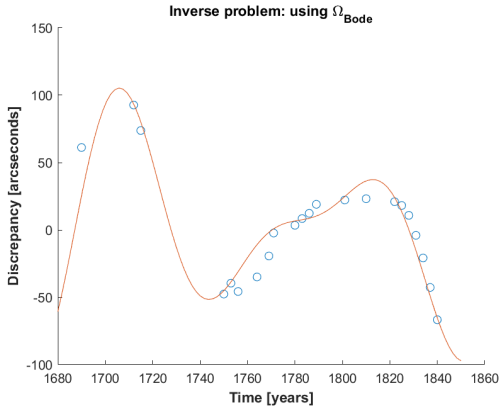

Figure 22: $\Delta\phi_{th}$ with Ω_{Bode} fitted to the historical data with varied t_0 and γ. Here $\gamma = -50.1712''$ and $t_0 = 1811.3643$.

This is quite a close fit which yields $\gamma = -50.1712''$ and $t_0 = 1811.3643$. Notice that in the inverse problem, the value of γ is more consistent with the range of values of the measured discrepancies than in the forward problem.

4.2.2 Vary Ω_N

In this case, Ω_N is a parameter when we fit the data to the theoretical discrepancy. Thus, we vary $\Omega = \Omega_U - \Omega_N$ to the data. We obtain the following fit in Figure 23:

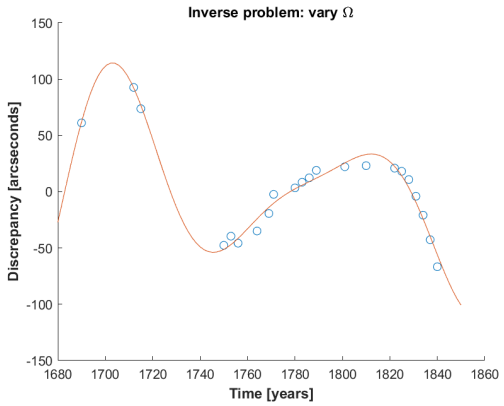

Figure 23: $\Delta\phi_{th}$ with varied Ω_N fitted to the historical data with varied t_0 and γ. Here $\Omega = 0.04270$, $t_0 = 1817.0182$ and $\gamma = -100.0911''$. This is the best fit to the inverse problem.

We immediately see that this is the closest fit so far. We have $t_0 = 1817.0182$, $\gamma = -100.0911$ and $\Omega = 0.04270$ rad per year, which corresponds to $\Omega_{fit,N} = \Omega_U - \Omega = 0.07479 - 0.04270 = 0.03209$ rad per year. The actual Neptune frequency is $\Omega_N = 0.03813$ rad per year. Thus, there is quite a difference between the actual Neptune frequency Ω_N and the fitted frequency, but a smaller difference than between $\Omega_{Bode,N}$ and Ω_N.

4.3 Root-Mean-Square Errors

In this section, we consider the root-mean-square errors [4] of the two cases previously discussed.

4.3.1 Using Ω_{Bode}

We first consider the root-mean-square error for different values of γ. The error plots for γ are symmetric around the D^2-axis. Thus, only considering the positive direction is enough. In Figure 24, we plotted the error against γ:

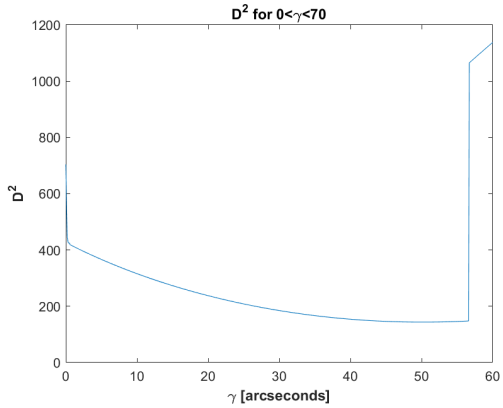

Figure 24: The root-mean-square error D^2 for different values of γ where for every γ the discrepancy $\Delta\phi_{th}$ with Ω_{Bode} is fitted to the data. We varied t_0. The error is parabola shaped at first and makes a jump around $\gamma \approx 57''$. The minimum is $D^2 = 143.7586$ attained at $\gamma = 50.1712''$.

The minimum is attained at $\gamma = 50.1712''$. We also notice an abrupt jump in D^2 around $\gamma \approx 57$" as expected. Earlier, we observed that the overall look of the fits changed drastically around that value.
Furthermore, we consider the error plot for different values of t_0 in Figure 25.

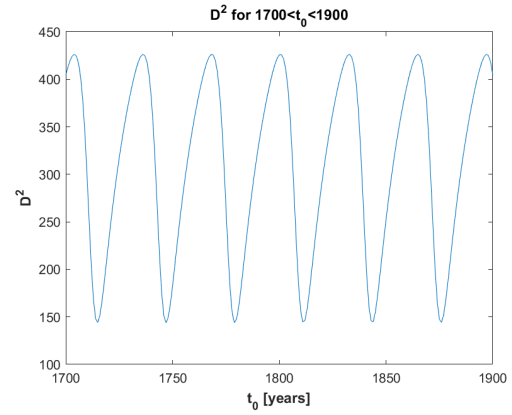

Figure 25: The root-mean-square error D^2 for different values of t_0 where for every t_0 the discrepancy $\Delta\phi_{th}$ with Ω_{Bode} is fitted to the data. The error is periodic and the minimum closest to 1822 is $D^2 = 143.7586$ at $t_0 = 1811.3643$.

In the figure, we observe the expected periodicity. The minimum error is $D^2 = 143.7586$ with $\gamma = -50.1712''$ and $t_0 = 1811.3643$.

4.3.2 Vary Ω_N

In this section, we calculate the root-mean-square error for different values of Ω. We plotted this in Figure 26.

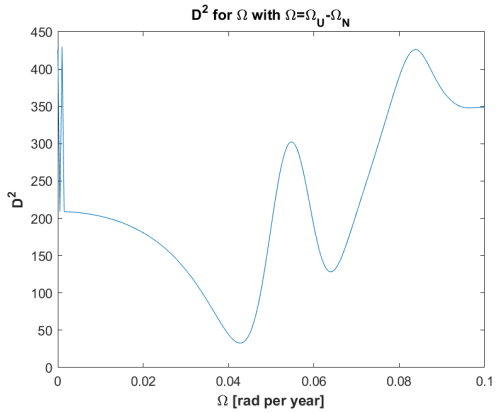

Figure 26: The root-mean-square error D^2 for different values of Ω where for every Ω the discrepancy $\Delta\phi_{th}$ is fitted to the data. The error attains some local minima and the global minimum is $D^2 = 32.7424$ at $\Omega = 0.0427$.

We observe several local minima and the global minimum at $\Omega = 0.0427$ with $\Omega_N = \Omega_{fit,N} = 0.03209$. Near zero the error behaves chaotically, that is why we observe the jump. The error at $\Omega = 0.0427$ is $D^2 = 32.7424$. This is the lowest error we have encountered and thus the best fit to the inverse problem. We can clearly see this when comparing Figure 22 and Figure 23.

4.4 Predicted Location

In this section, we calculate the location of Neptune for the two different cases described in this chapter. We use the optimal values for t_0 and Ω_N from the previous sections to achieve this. We calculate the angle between the actual and predicted location in 1846, the year Neptune was discovered. Recall that $\Omega \times \Delta t$ equals the number of radians travelled by a certain planet in a time span Δt. We derive a formula, Δ_N, for the difference between the actual location and the predicted location as follows.

- The actual location of Neptune in 1846 is the location in 1822 plus $24 \times \Omega_N$.
- The theoretical location of Neptune is the location of Uranus at t_0 plus $(1846 - t_0) \times \Omega_N$. The location of Uranus in t_0 is equal to the location in 1822 plus $(t_0 - 1822) \times \Omega_U$.

We take the difference of the preceding expressions. Notice that the location in 1822 cancels out. We obtain the following expression for Δ_N:

$$\Delta_N = |24\Omega_N - (t_0 - 1822)\Omega_U - (1846 - t_0)\widetilde{\Omega}_N| \tag{33}$$

where $\widetilde{\Omega}_N \in \{\Omega_{Bode,N}, \Omega_{fit,N}\}$. We calculate this difference Δ_N for the varied $\Omega_{fit,N}$ and $\Omega_{Bode,N}$.

4.4.1 Using Ω_{Bode}

In this case, the optimal value for the time of conjunction is $t_0 = 1811.3643 \approx 1811$. Thus, Δ_N becomes:

$$\Delta_N = |24\Omega_N + 11\Omega_U - 35\widetilde{\Omega}_{Bode,N}| = 0.8278975 \text{ rad} \tag{34}$$

4.4.2 Vary Ω_N

In this case, the optimal value for the time of conjunction is $t_0 = 1817.0182 \approx 1817$. Thus, Δ_N becomes:

$$\Delta_N = |24\Omega_N + 5\Omega_U - 29\widetilde{\Omega}_{fit,N}| = 0.35846 \text{ rad} \tag{35}$$

The predictions from our derived t_0 and Ω_N are not as close as we would expect from the fits in the previous sections. We think we lost some valuable information along the way by making the Uranus-Neptune model too easy. For example, both Le Verrier and Adams did include non-zero eccentricities in their calculations. Perhaps something like this is necessary in order to get a more accurate result. For more detailed information about the predictions of Le Verrier and Adams, we refer one to [3] and [2].

4.5 Conclusion Inverse Problem

We used Bode's law to calculate Ω_{Bode} and used this to fit $\Delta\phi_{th}$ to the data. Afterwards, we varied Ω_N. From their respective root-mean-square errors, we conclude that the latter allows for a more accurate result. Besides, the inverse problem has a better fit to the problem than the forward problem. Eventually, we calculated the difference between the predicted and actual Neptune location, Δ_N. For $\Omega_{Bode,N}$, we got $\Delta_N = 0.8278975$ rad and for $\Omega_{fit,N}$, we got $\Delta_N = 0.35846$ rad. Unfortunately, this is much more than the 1° error of Urbain Le Verrier [3]. We think this is due to the simplified Sun-Uranus-Neptune system we considered. We must have lost some valuable information.

Regarding the results in [4], we again observe a smaller D^2 in [4] due to similar reasons as described in the forward problem.

5 Conclusion

In the previous chapters, we have taken a look at the forward and inverse problem [4]. From the equations of motion of Uranus, we derived an expression for the theoretical perturbations $\Delta\phi_{th}$ [4]. Afterwards, we fitted $\Delta\phi_{th}$ to the historical discrepancy. Using the root-mean-square error, we compared the results. The best fit to the forward problem was when we varied both γ and t_0. In particular, varying γ had a major impact on the D^2 error. As for the inverse problem, we first used Ω_{Bode} and then we varied Ω. The latter led to the best fit to the inverse problem as well as the best fit to the data in general. From these fits, we obtained optimal values for t_0 and Ω_N. We calculated the predicted location of Neptune from these values. Our best prediction is 0.35846 rad away from the actual location in 1846. Le Verrier [3] predicted the location of Neptune within 1°, this is extraordinarily close to the actual location. The Neptune-Uranus system we used is a simplified version of reality. Hence, we did not get such an accurate prediction. Unfortunately, we must have lost some valuable information, even though the fits seemed close to the data.

Bibliography

[1] B. Ryden and B. M. Peterson. *Foundations of astrophysics*. Cambridge University Press, 2020.

[2] J. C. Adams. "An Explanation of the Observed Irregularities in the Motion of Uranus." In: *Memoirs of the Royal Astronomical Society* 16 (1847), p. 427.

[3] J. Laskar. "Des premiers travaux de Le Verrier à la découverte de Neptune". In: *Comptes Rendus Physique* 18.9-10 (2017), pp. 504–519.

[4] H. M. Lai, C. C. Lam, and K. Young. "Perturbation of Uranus by Neptune: A modern perspective". In: *American Journal of Physics* 58.10 (1990), pp. 946–953.

[5] H. D. Young et al. *University physics*. Vol. 9. Addison-Wesley Reading, MA, 1996.

[6] R. A. Lyttleton. "A short method for the discovery of Neptune". In: *Monthly Notices of the Royal Astronomical Society* 118.6 (1958), pp. 551–559.